

Quasiclassical theory of laser-induced atomic-beam dispersion

E. Arimondo

Istituto di Fisica della Università di Pisa, Piazza Torricelli 2, I-55100 Pisa, Italy

A. Bambini

Istituto di Elettronica Quantistica del Consiglio Nazionale delle Ricerche, via Panciatichi 56/30 I-50127 Firenze, Italy

S. Stenholm

Research Institute for Theoretical Physics, University of Helsinki, Siltavuorenpenger 20 C SF-00170 Helsinki 17, Finland

(Received 24 September 1980)

We present a theoretical model for the interaction of a beam of two-level atoms with a resonant laser beam. It is shown that the radiation force, while averaging to zero at resonance, produces a transverse spread of the atomic velocities. If radiative damping is ignored, this spread increases linearly with time and finally saturates towards a steady value. Although the spread has a quantum-mechanical origin, we show that it is possible, in the limit $\hbar k \rightarrow 0$, to describe the phenomenon in terms of differential equations of motion for the atomic translational variables, as in the classical case. In this model it is also possible to describe the effects of radiative damping, as well as other additional effects, which may occur in a real experiment. Finally a comparison of our results with experimental data, recently obtained on an Na atomic beam, has been made. Although an order-of-magnitude fit of the experimental data could be obtained, the weights of the different causes, reducing the spread, were found to be ambiguous and have been left partly open.

I. INTRODUCTION

The subject of the atomic motion in a resonant or nearly resonant electromagnetic field has recently attracted much attention because of its important applications, such as, for instance, the selection of atomic species in an atomic beam¹ (isotope separation) and cooling and trapping of atoms.² The trajectory of an atom can be affected by its interaction with an electromagnetic field through several processes: a lenslike effect caused by an inhomogeneity of a standing-wave field, fluctuations in spontaneous or stimulated emission of radiation after an excitation by a resonant field, and recoil effects in spontaneous emission processes. The spread of an atomic beam in the presence of an inhomogeneous radiofrequency field was observed for potassium atoms by Bloom *et al.*,³ and for CsF molecules by Hill *et al.*⁴ Deflection of Na atoms by an intensity gradient of an optical laser beam was observed by Bjorkholm *et al.*,⁵ while the modification of a laser beam propagation because of the gradient forces was detected by Tam and Happer.⁶ The force exerted on the atoms in these conditions is usually referred to as the gradient force. Deflection of atoms caused by momentum transfer through the excitation by a traveling optical wave was detected in an early experiment with conventional sources⁷ and later with laser sources by several investigators.⁸ Also, the velocity dependent force exerted by a traveling wave on resonant ions has been used to cool and

retain ions in a trap.⁹ In these cases, the force is referred to as a radiation pressure force. If the atoms interact with a standing-wave field, made up of two oppositely traveling waves, the radiation pressure force at resonance is zero, since an atom can as well interact with the one or the other traveling wave, and therefore the average momentum transferred in these processes is zero. In this case, however, quantum fluctuations of the induced processes occur and cause a spread of the atomic trajectories. This process can be related to the scattering process of electrons in a standing-wave pattern (the so-called Kapitza-Dirac effect¹⁰), although in the latter effect the scattered particles have no internal degrees of freedom. The spread of an atomic beam interacting with a standing-wave laser field has been investigated by Arimondo *et al.*¹¹ Letokhov and co-workers¹² have proposed the trapping of atoms in the antinodes of a near-resonant standing-wave laser field. Different theoretical models based on semiclassical or quantum-mechanical treatments of the translational degrees of freedom of the atoms have been developed in recent years.¹³ Among the cases treated, we mention the quantum-mechanical spread of an atomic beam interacting with a traveling wave field¹⁴ or with a standing-wave field¹⁵; or the classical force exerted on the atoms interacting with a plane traveling wave or a plane standing wave.¹⁶ In a recent series of papers, Cooks has treated several aspects¹⁷ of the problem, with the ultimate goal of unifying

the various treatments existing in the literature.¹⁸ A very recent paper has treated the atomic motion by quantum noise theory.¹⁹

Although in the discussion above we have distinguished the two cases of atomic motion in an inhomogeneous resonant field and in a plane, standing-wave field, both these cases are manifestations of the same effect, namely the quantum-mechanical splitting of atomic trajectories in a classical, nonuniform field. In the first case, nonuniformity comes from variations of the electromagnetic field amplitude across a Gaussian-shaped laser beam, while in the second case nonuniformity is provided by the standing-wave pattern of the field. The effect of splitting of the trajectories in a nonuniform field is referred to as an optical Stern-Gerlach effect²⁰ (OSGE). It is the aim of this paper to show how it is possible to calculate the atomic-beam trajectories in the case in which the momentum transferred from the field to the atoms is much smaller than a typical atomic momentum (the quasiclassical limit); this case turns out to be of practical interest, since in most experimental situations the conditions for the applicability of the quasiclassical limit are well satisfied. We want also to show how it is possible to introduce in our model several additional features which are present in actual experiments, such as, for instance, the modifications introduced by the random interruptions of the phase coherence caused by spontaneous emission processes or the effects of a standing-wave Gaussian-shaped laser beam. We compare also the experimental data on the spread of an atomic beam in the presence of a standing-wave pattern, obtained by Arimondo *et al.*¹¹ with the OSGE calculations. We show that their results cannot be interpreted as a pure OSGE, since other effects interfere and affect considerably the experiment. In Sec. II we present, for the sake of completeness, the quantum-mechanical equations of motion for the OSGE. The density-matrix equations and their quasiclassical limit are discussed in Sec. III. In the same section we also show the quasiclassical calculation contrasted with the quantum-mechanical ones, and we see that significant deviations of the former case from the latter do not occur under practical laboratory conditions. In Sec. IV we present the quasiclassical calculations for the experiment of Arimondo *et al.*; the evaluated curve for a pure OSGE does not fit the experimental data, since the actual spread of the atomic beam is considerably smaller than in the idealised situation. Some additional features are then added to the pure OSGE to make the theory fit the experimental points. This is done in Sec. V, in which

we show how these effects affect the spread of the atomic beam. Finally, in Sec. VI, we draw some conclusions and discuss the case treated in this article.

The equations of the OSGE quantum-mechanical and semiclassical descriptions are very similar to those obtained in the nonrelativistic theory of the free-electron laser.²¹ Thus few arguments, not relevant to the atomic-beam experiment and discussed in that context, will not be repeated here.

II. DERIVATION OF THE OSGE EQUATIONS

Let us idealize the experimental situation as shown in Fig. 1. The atomic beam is perfectly collimated and the atomic momentum has only a longitudinal component, p_z , before entering the interaction region. The laser field is made up of two oppositely running plane waves, $\frac{1}{2}E_0 \cos(\omega t - kx)$ and $\frac{1}{2}E_0 \cos(\omega t + kx)$, linearly polarized along the \hat{y} direction and traveling in the \hat{x} direction. They form, therefore, a standing-wave pattern, which is the cause of the Stern-Gerlach-type spread of the atomic beam. The electric field amplitude is assumed to be constant within a slab of thickness d in the z direction and zero elsewhere. The field frequency ω is tuned to the atomic transition frequency $\omega_0 = (E_a - E_b)/\hbar$ between the ground level b and the excited level a .

From a classical point of view, the atoms do not experience any force in the radiation field; at resonance the field induces a dipole moment in the atom which oscillates 90° out-of-phase with respect to the inducing field. Under ordinary experimental conditions, the optical period T is very short compared with the time characteristic of the rate of change of momentum. Therefore the atom has a constant momentum during an optical period and, averaging over T , we obtain that the mean potential energy of the atom is zero, independently of the position of the atom in the standing-wave pattern. The same result is obtained if we quantize the internal degrees of freedom of the atom, but leave the center-of-

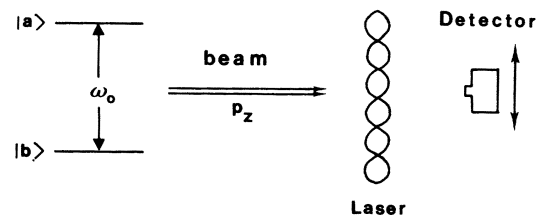


FIG. 1. Frame of reference and setup of a typical experiment with the atomic beam, the laser standing wave, and the detection apparatus.

mass velocity as a classical variable. This has been shown recently by Cook.¹⁷ To account for the spread of the atomic beam in the resonant standing-wave optical field, we therefore need to quantize both the internal degrees of freedom and the center-of-mass motion of the atom.

For the one-dimensional problem, the Hamiltonian of a two-level atom in a standing-wave electromagnetic field is given by

$$H = \frac{1}{2m} p^2 + \frac{1}{2} \hbar \omega_0 \sigma_3 - \hbar \Omega (\sigma^+ + \sigma^-) \cos \omega t \cos kx, \quad (1)$$

where p is the atomic momentum along the x direction,

$$\Omega = \frac{\hbar \mathcal{E}_0}{\hbar} \quad (2)$$

is the Rabi flipping frequency, σ_1 , σ_2 , and σ_3 are the Pauli operators associated with the two-level system, and

$$\sigma^\pm = \frac{1}{2} (\sigma_1 \pm i \sigma_2). \quad (3)$$

To eliminate the rapid oscillations at the optical frequency in the equations of motion, we transform to the interaction picture

$$|\psi_I(t)\rangle = U(t) |\psi_S(t)\rangle, \quad (4)$$

where

$$U(t) = \exp(i \omega \sigma_3 t / 2). \quad (5)$$

Then the Schrödinger equation can be written

$$i \hbar \frac{d}{dt} |\psi_I\rangle = \left(\frac{1}{2m} p^2 + \frac{\hbar}{2} (\omega_0 - \omega) \sigma_3 - \frac{\hbar \Omega}{2} (\sigma^+ + \sigma^-) \cos kx \right) |\psi_I(t)\rangle, \quad (6)$$

where the rapidly oscillating terms at twice the optical frequency have been omitted (the rotating-wave approximation). In the p representation the wave function can be written as

$$|\psi_I(p, t)\rangle = a(p, t) |a\rangle + b(p, t) |b\rangle. \quad (7)$$

Then the operator p^2 acts on $a(p, t)$ and $b(p, t)$ as a multiplier, while the operator $\cos kx$ acts as a translator

$$\begin{aligned} (\cos kx) \alpha(p, t) &\equiv \frac{1}{2} (e^{ikx} + e^{-ikx}) \alpha(p, t) \\ &= \frac{1}{2} [\alpha(p + \hbar k, t) + \alpha(p - \hbar k, t)] \\ \alpha &= a, b. \end{aligned} \quad (8)$$

Projecting Eq. (6) onto $|a\rangle, |b\rangle$, we have

$$i \hbar \frac{\partial a}{\partial t} = \frac{p^2}{2m} a + \frac{\hbar}{2} (\omega_0 - \omega) a - \frac{\hbar \Omega}{4} [b(p + \hbar k, t) + b(p - \hbar k, t)], \quad (9)$$

$$i \hbar \frac{\partial b}{\partial t} = \frac{p^2}{2m} b - \frac{\hbar}{2} (\omega_0 - \omega) b - \frac{\hbar \Omega}{4} [a(p + \hbar k, t) + a(p - \hbar k, t)].$$

At resonance, $\omega = \omega_0$, these equations can be decoupled by means of the replacement of a, b with α, β defined as

$$\begin{aligned} \alpha &= \frac{1}{\sqrt{2}} (a + b), \\ \beta &= \frac{1}{\sqrt{2}} (a - b). \end{aligned} \quad (10)$$

Then the equations for α, β read

$$\begin{aligned} i \hbar \frac{\partial \alpha}{\partial t} &= \frac{p^2}{2m} \alpha - \frac{\hbar \Omega}{4} [\alpha(p + \hbar k, t) + \alpha(p - \hbar k, t)], \\ i \hbar \frac{\partial \beta}{\partial t} &= \frac{p^2}{2m} \beta + \frac{\hbar \Omega}{4} [\beta(p + \hbar k, t) + \beta(p - \hbar k, t)]. \end{aligned} \quad (11)$$

These equations show that the wave function of the atoms splits into two mutually independent components which evolve in time under the action of the potential energies $-\frac{1}{2} \hbar \Omega \cos kx$ and $+\frac{1}{2} \hbar \Omega \cos kx$, respectively. The wave function of an atom, originally in its ground state, has equal components α and β . Therefore the single-atom components are split under the action of the electromagnetic field inhomogeneity¹³; hence the name optical Stern-Gerlach effect. We will see in the next section how to pass from the quantum problem to an apparently classical one, in the limit $\hbar k \rightarrow 0$. Now we want to show under what conditions Eqs. (9) can be solved in terms of known functions, and to obtain a method for the evaluation of the solution in the general case.

Let us consider the case in which the atomic sample has been prepared in a well collimated monochromatic beam, propagating along the z axis. Then the initial state for the incoming atoms is a plane wave, with perfectly defined momentum and total undetermination of the position of the atoms. The initial momentum along the x direction is zero. Momentum transfer from the field to atoms occurs in integral multiples of $\hbar k$. Therefore $a(p, t)$ and $b(p, t)$ in (9) can be expressed as the discrete series

$$a(p, t) = \hbar k \sum_n a_n(t) \delta(p - n \hbar k), \quad (12a)$$

$$b(p, t) = \hbar k \sum_n b_n(t) \delta(p - n \hbar k), \quad (12b)$$

with the initial conditions, at time $t=0$ when the atoms enter the interaction region

$$\begin{aligned} a_n(0) &= 0, \\ b_n(0) &= 1, \end{aligned}$$

since the atoms are initially in their ground state. One can also easily see that the sum in (12a) ranges over odd values of n , while (12b) ranges over even values of n . Therefore, setting

$$x_n(t) = \begin{cases} a_n(t), & \text{for } n \text{ odd} \\ b_n(t), & \text{for } n \text{ even} \end{cases} \quad (13)$$

we obtain from (9) an infinite set of differential-difference equations

$$i\hbar \frac{dx_n}{dt} = \frac{n^2 \hbar^2 k^2}{2m} x_n(t) - \frac{\hbar\Omega}{4} [x_{n+1}(t) + x_{n-1}(t)], \quad (14)$$

with

$$x_n(0) = \delta_{0,n}. \quad (15)$$

Equations (14) can be solved in terms of known analytical functions if the interaction time is so short that only a few translational states are reached (starting from the state $n=0$) by the atoms, and for those states the kinetic energy $n^2 \hbar^2 k^2 / 2m$ is negligible compared with the interaction energy $\hbar\Omega/4$. Then one can see that the solution to (14), (15), when the kinetic energy terms are ignored, is given by²²

$$x_n(t) = i^n J_n(\Omega t/2), \quad (16)$$

where J_n is the Bessel function of integer order. Therefore, after an interaction time τ , $2n_{\max}$ translational states are occupied, with

$$n_{\max} \sim \Omega \tau / 2, \quad (17)$$

and the probability distribution $|x_n|^2$ has its maximum value just around n_{\max} . Using Eqs. (16), the spread of transverse momentum $\langle p^2 \rangle$ can be easily evaluated giving

$$\langle (p^2) \rangle^{1/2} = \left[\hbar^2 k^2 \sum_n n^2 J_n^2 \left(\frac{\Omega t}{2} \right) \right]^{1/2} = \frac{\hbar k \Omega \tau}{2\sqrt{2}}. \quad (18)$$

Then we see that the atomic spread in the transverse direction increases linearly with the interaction time, and, also, depends linearly on Ω , i.e., on the electric field amplitude of the laser beam. Increasing the interaction time τ , a situation is reached in which translational states of the atoms are occupied for which the kinetic

energy is comparable with the interaction energy. Therefore, when $p^2/2m \sim \hbar\Omega/4 = \hbar \mathcal{E}_0/4$, the probability amplitudes x_n are no longer expressed by Eqs. (16). To our knowledge no analytical solution of Eqs. (14) exists and a numerical integration must be carried out in order to obtain the actual probability distribution of translational states.²¹

So far we have described the quantum-mechanical treatment of the OSGE; under the action of a nonuniform electromagnetic field the wave function of each single atom of the beam is split symmetrically; the average transverse momentum of the atoms is still zero, but α and β describe two trajectories symmetrically spread around the unperturbed path. The whole process is a coherent one; no phase-interruption mechanism, such as spontaneous decay processes or phase fluctuations in the laser beam have been introduced. The full quantum process, therefore, would require keeping all terms in Eqs. (16). We will show, in the next section, how we can avoid such a time consuming calculation, just retaining the characteristic features of the OSGE, and discarding all quantum effects which would be difficult—if not impossible—to detect.

III. DENSITY MATRIX EQUATIONS AND THE QUASICLASSICAL LIMIT

A. Theory

The density-matrix description is carried out in the representation (10). Indeed, the states $|\alpha\rangle, |\beta\rangle$, defined as

$$|\alpha\rangle = \frac{1}{\sqrt{2}} (|a\rangle + |b\rangle), \quad (19)$$

$$|\beta\rangle = \frac{1}{\sqrt{2}} (|a\rangle - |b\rangle), \quad (20)$$

are eigenstates of the operator $\sigma_1 = \sigma^+ + \sigma^-$ which appears in (6),

$$\sigma_1 |\alpha\rangle = |\alpha\rangle, \quad (21)$$

$$\sigma_1 |\beta\rangle = -|\beta\rangle.$$

In this representation, the equation of motion for the density matrix $\hat{\rho}(x_1, x_2, t)$ describing both the internal and the translational degrees of freedom is given by

$$i\hbar \frac{\partial}{\partial t} \hat{\rho}(x_1, x_2, t) = -\frac{\hbar^2}{2m} \left(\frac{\partial^2}{\partial x_1^2} - \frac{\partial^2}{\partial x_2^2} \right) \hat{\rho}(x_1, x_2, t) + \frac{\hbar\Omega}{2} \left[\cos kx_1 \begin{pmatrix} 1 & 0 \\ 0 & -1 \end{pmatrix} \hat{\rho}(x_1, x_2, t) - \cos kx_2 \hat{\rho}(x_1, x_2, t) \begin{pmatrix} 1 & 0 \\ 0 & -1 \end{pmatrix} \right], \quad (22)$$

where

$$\hat{\rho}(x_1, x_2, t) = \begin{pmatrix} \rho_{\alpha\alpha}(x_1, x_2, t) & \rho_{\alpha\beta}(x_1, x_2, t) \\ \rho_{\beta\alpha}(x_1, x_2, t) & \rho_{\beta\beta}(x_1, x_2, t) \end{pmatrix}. \quad (23)$$

In a normal Stern-Gerlach experiment, the off-diagonal elements of the density matrix are zero before the interaction with the magnetic field, because the atoms have equal probability to be

spin up or spin down, independently of the direction of the axis of quantization. In our actual problem, however, this is not the case. Since at $t=0$ the atoms are in their ground state, $|\beta\rangle$, the two states $|\alpha\rangle$ and $|\beta\rangle$ have, at $t=0$, the same population $\frac{1}{2}$ (as in a normal Stern-Gerlach experiment), but there is complete coherence between them. We shall see, however, that coherence effects are negligible in the quasiclassical limit.

Introducing the center of mass X and relative coordinate x ,

$$X = \frac{1}{2}(x_1 + x_2), \quad (24)$$

$$x = x_1 - x_2, \quad (25)$$

we find the equations for $\hat{\rho}(X, x, t)$

$$\begin{aligned} i \frac{\partial}{\partial t} \rho_{\alpha\alpha} &= -\frac{\hbar}{m} \frac{\partial}{\partial x} \frac{\partial}{\partial X} \rho_{\alpha\alpha} - \Omega \sin \frac{kx}{2} \sin kX \rho_{\alpha\alpha}, \\ i\hbar \frac{\partial}{\partial t} \rho_{\beta\beta} &= -\frac{\hbar}{m} \frac{\partial}{\partial x} \frac{\partial}{\partial X} \rho_{\beta\beta} + \Omega \sin \frac{kx}{2} \sin kX \rho_{\beta\beta}, \\ i\hbar \frac{\partial}{\partial t} \rho_{\alpha\beta} &= -\frac{\hbar}{m} \frac{\partial}{\partial x} \frac{\partial}{\partial X} \rho_{\alpha\beta} + \Omega \cos \frac{kx}{2} \cos kX \rho_{\alpha\beta}, \\ i\hbar \frac{\partial}{\partial t} \rho_{\beta\alpha} &= -\frac{\hbar}{m} \frac{\partial}{\partial x} \frac{\partial}{\partial X} \rho_{\beta\alpha} - \Omega \cos \frac{kx}{2} \cos kX \rho_{\beta\alpha}. \end{aligned} \quad (26)$$

To perform the passage to the quasiclassical limit in the translational degrees of freedom of the atoms, it is convenient to introduce the Wigner representation of the density matrix

$$\hat{\rho}(X, P, t) = \frac{1}{\sqrt{2\pi}} \int_{-\infty}^{+\infty} e^{-iPx/\hbar} \hat{\rho}(X, x, t) dx, \quad (27)$$

which satisfies the set of (uncoupled) differential equations

$$\begin{aligned} \frac{\mathcal{D}}{\mathcal{D}t} \rho_{\alpha\alpha}(X, P, t) &= -\frac{\Omega}{2} \sin kX \left[\rho_{\alpha\alpha} \left(X, P + \frac{\hbar k}{2}, t \right) \right. \\ &\quad \left. - \rho_{\alpha\alpha} \left(X, P - \frac{\hbar k}{2}, t \right) \right], \\ \frac{\mathcal{D}}{\mathcal{D}t} \rho_{\beta\beta}(X, P, t) &= \frac{\Omega}{2} \sin kX \left[\rho_{\beta\beta} \left(X, P + \frac{\hbar k}{2}, t \right) \right. \\ &\quad \left. - \rho_{\beta\beta} \left(X, P - \frac{\hbar k}{2}, t \right) \right], \\ \frac{\mathcal{D}}{\mathcal{D}t} \rho_{\alpha\beta}(X, P, t) &= -\frac{i\Omega}{2} \cos kX \left[\rho_{\alpha\beta} \left(X, P + \frac{\hbar k}{2}, t \right) \right. \\ &\quad \left. + \rho_{\alpha\beta} \left(X, P - \frac{\hbar k}{2}, t \right) \right], \\ \frac{\mathcal{D}}{\mathcal{D}t} \rho_{\beta\alpha}(X, P, t) &= \frac{i\Omega}{2} \cos kX \left[\rho_{\beta\alpha} \left(X, P + \frac{\hbar k}{2}, t \right) \right. \\ &\quad \left. + \rho_{\beta\alpha} \left(X, P - \frac{\hbar k}{2}, t \right) \right], \end{aligned} \quad (28)$$

where we have introduced the differential operator

$$\frac{\mathcal{D}}{\mathcal{D}t} \equiv \frac{\partial}{\partial t} + \frac{P}{m} \frac{\partial}{\partial X}. \quad (29)$$

We are now in a position to take the quasiclassical limit in Eqs. (28). Expanding the right-hand sides (rhs) of Eqs. (28) in powers of $\hbar k$, and keeping only the terms linear in $\hbar k$, we obtain for the diagonal elements $\rho_{\alpha\alpha}, \rho_{\beta\beta}$

$$\frac{\mathcal{D}}{\mathcal{D}t} \rho_{\alpha\alpha}(X, P, t) = -\frac{\hbar k \Omega}{2} \sin kX \frac{\partial}{\partial P} \rho_{\alpha\alpha}(X, P, t), \quad (30)$$

$$\frac{\mathcal{D}}{\mathcal{D}t} \rho_{\beta\beta}(X, P, t) = \frac{\hbar k \Omega}{2} \sin kX \frac{\partial}{\partial P} \rho_{\beta\beta}(X, P, t).$$

In so doing, we consider the kick received by the atom in each elementary process as an infinitesimal modification of the atomic momentum, thus regarding the atomic momentum as a continuous variable, instead of a discrete one like in Eqs. (28).

Equations (30) allow a remarkable interpretation of the process; indeed, since

$$-\hbar k \Omega \sin kX = -\hbar k \delta_0 \sin kX \equiv \frac{\partial W}{\partial X}, \quad (31)$$

where $W(X)$ is the classical potential energy of the atom in the electromagnetic field, Eqs. (30) describe the particle's trajectories in a Stern-Gerlach-type experiment under the influence of a gradient field; the trajectories of particles in the α and in the β states split.

In our process, however, the gradient field is periodic in space; therefore a space translation of one-half wavelength would change trajectories of α states into trajectories of β states, and vice versa. Furthermore, the particles have been assumed to enter the interaction region with a sharp distribution in transverse momentum; i.e., they have a wide (much larger than $2\pi/k$) distribution in X . Therefore, when replacing the diagonal density matrix elements with a statistical ensemble of classical particles, we have to introduce a broad distribution in the transverse coordinate X . This means that the characteristics of Eqs. (30) which describe the classical trajectories have their initial points distributed over a region much larger than $2\pi/k$. With these initial conditions, the α -state and β -state trajectories will differ only by an unessential shift in their starting point. This difference will of course disappear in the averaging over the statistical ensemble.

The characteristics of Eqs. (30) are given by the set of differential equations

$$m \frac{dX}{dt} = P, \quad (32)$$

$$\frac{dP}{dt} = \frac{\hbar k \Omega}{2} \sin kX,$$

where the \pm signs in front of $\frac{1}{2} \hbar k \Omega \sin kX$ has been dropped in view of the above discussion. Equations (32) describe the motion of a particle in a periodic potential; they are pendulum equations. Integration of Eqs. (32) is much simpler than the method based on Eqs. (14) of Sec. II, and the results are very close; as will be shown in the next section, the only difference is a ripple in the probability distribution which can hardly be detected in experiments.

We consider now the quasiclassical limit of the other equations, i.e., the equations for the off-diagonal elements $\rho_{\alpha\beta}$ and $\rho_{\beta\alpha}$. Here the coefficient of the linear term is zero. We are therefore left with

$$\frac{\mathcal{D}}{\mathcal{D}t} \rho_{\alpha\beta} = -i\Omega \cos kX \rho_{\alpha\beta}, \quad (33)$$

$$\frac{\mathcal{D}}{\mathcal{D}t} \rho_{\beta\alpha} = i\Omega \cos kX \rho_{\beta\alpha}$$

[note that \hbar , being contained in Ω , does not disappear from (33) as it does in Eq. (30) because of (31)].

The atomic momentum P enters Eqs. (33) as a parameter because the operator $\partial/\partial P$ does not appear. The characteristics of Eqs. (33) are therefore straight lines, starting at $X=X_0$ (with X_0 being within the range of the initial conditions), and $P=P(0)=0$. We are led to the following conclusion: In the quasiclassical limit the "coherence" $\rho_{\alpha\beta}, \rho_{\beta\alpha}$ between α states and β states cannot be defined for particles which undergo deflections by the gradient field. This fact can be interpreted in simple terms: Strictly speaking, the classical limit of the motion of the atom can be carried out only if the deBroglie wavelength of the atom is small compared with the wavelength of the electromagnetic field, i.e., $P \gg \hbar k$. In the limit $\hbar k \rightarrow 0$, however, this is true for all particles, save for those which are not deflected, i.e., for those particles which keep their zero transverse momentum. Thus coherence, which is a quantum-mechanical feature, survives for these particles only. This is the classical reminiscence of the quantum-mechanical forward diffraction cone in which the incoming coherence survives.

Within this simple quasiclassical model it is possible to discuss all the effects of spontaneous emission processes on the spread of the atomic

beam (see Appendix A). Other effects will be discussed as well in the next sections.

B. Numerical calculations

We have performed numerical calculations on the fully quantum-mechanical equations [Eqs. (14)], and on their corresponding quasiclassical analog [Eqs. (32)]. Introducing the recoil kinetic energy ϵ in units of angular frequency,

$$\epsilon = \hbar k^2 / 2m, \quad (34)$$

and an interaction time in dimensionless units,

$$\tau = \epsilon t, \quad (35)$$

we find that both Eqs. (14) and (33) scale with the same factor, Ω/ϵ , i.e., the ratio between the interaction energy Ω and the recoil kinetic energy ϵ . Indeed, Eqs. (14) can be written as

$$i \frac{d}{d\tau} x_n = n^2 x_n - \frac{\Omega}{4\epsilon} [x_{n+1}(\tau) + x_{n-1}(\tau)], \quad (36)$$

while Eqs. (32) become

$$\frac{d\xi}{d\tau} = 2Q, \quad (37)$$

$$\frac{dQ}{d\tau} = \frac{\Omega}{2\epsilon} \sin \xi, \quad (38)$$

with

$$Q = P/\hbar k, \quad (39)$$

$$\xi = kX.$$

Figure 2 shows the probability distribution $|x_n|^2$, as a function of n , obtained from a numerical integration of (36), and the probability distribution $f(\bar{Q})$ obtained from the quasiclassical Eqs. (37) and (38). The latter one has been evaluated

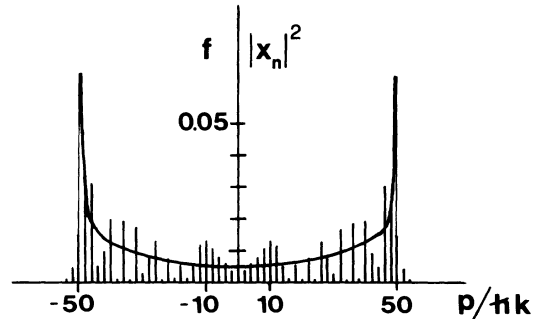


FIG. 2. The momentum distribution of the OSGE. The continuous curve is obtained from a quasiclassical calculation, while the discrete spectrum is obtained from the fully quantum-mechanical calculation. The two spectra are obtained with $\Omega t / 2 = 50$ and $\Omega/\epsilon = 2 \times 10^4$. With these values the spread is in the linear regime of Eq. (16).

just by counting how many trajectories [from the whole set initiated at $\tau = 0$ with $\xi(0)$ ranging between 0 and 2π , and with $Q(0) = 0$] have at the final time τ reached a value of Q such that $\bar{Q} \leq Q \leq \bar{Q} + \Delta\bar{Q}$. We note that the parameter n becomes the variable Q in the limit $\hbar k \rightarrow 0$.

The two graphs in Fig. 2 show the quantum features which are missed when passing to the continuum. While the continuous line matches fairly well the discrete spectrum on the average, the ripples of the latter one, which are of quantum origin, are washed out. The maxima of the two distributions coincide, but the quantum distribution is different from zero (even if negligibly small) even in regions not allowed for the classical particles.²¹ Figure 3, curve (b), shows the spreads of the distribution as a function of τ (the averages, or the first moment, are zero in both cases due to the symmetry of the problem). Here the quasiclassical and fully quantum graphs coincide, and since the spread is what is actually detected in experiments, this shows the validity of the quasiclassical limit.

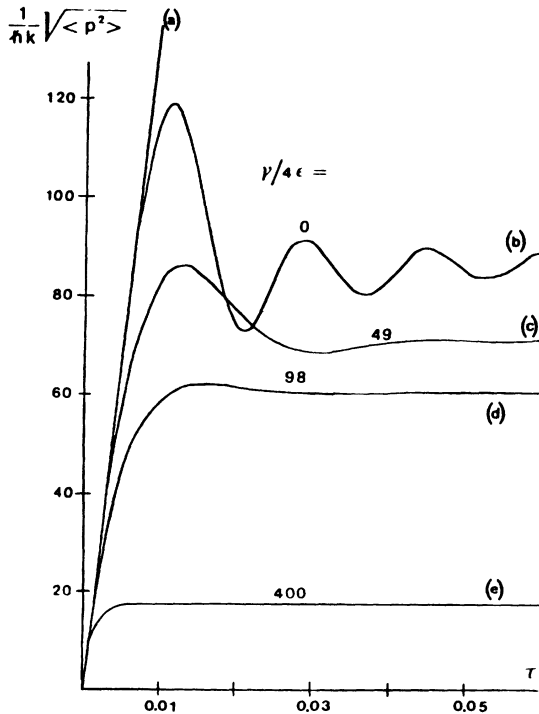


FIG. 3. Time evolution of the rms of the atomic momentum spread, measured in $\hbar k$ units. The Rabi flipping frequency is such that $\Omega/\epsilon = 4 \times 10^4$. In curve (a) the linear unsaturated spread is reported and in curve (b) the saturation regime is reached through damped oscillations. The curves (c), (d), and (e) are obtained in the presence of a damping mechanism with $\gamma/4\epsilon = 49$, 98, and 400, respectively.

It turns out that the spread increases linearly with time at the beginning [such very short τ for which Eq. (29) is valid], then the spread reaches saturation and, after some oscillations, tends towards a constant value. Saturation is reached for values of $\langle p^2 \rangle^{1/2}$ of the order of $\frac{1}{2} \hbar k \sqrt{\Omega/\epsilon}$, in agreement with the value derived by Cook and Bernhardt.¹⁵

IV. COMPARISON OF THE OSGE WITH EXPERIMENTAL DATA ON Na ATOMIC BEAM

The atomic spread of a Na beam interacting with an orthogonal standing-wave laser field was measured in Ref. 11 for several values of the laser power. The atomic beam was sent across a laser beam at normal incidence, and the spread was measured by detecting the number of atoms which were deflected from the longitudinal axis by the interaction with the field. We compare now the experimental results with the theoretical curve obtained in the preceding section, to establish whether the experiment can be interpreted as a pure OSGE.

To compare the experimental data with the OSGE curve, we need to know the values of the two parameters involved in the experiment, namely the Rabi flipping frequency Ω and the interaction time τ . The recoil kinetic energy ϵ can easily be evaluated in terms of the well-known Na atomic mass and the wave number of the resonant transition.

The Rabi frequency was evaluated in Ref. 11 by measuring also the spread of the atomic beam as a function of the detuning, $\omega - \omega_0$, of the laser frequency from the transition frequency, and assuming that the spread follows the usual saturation broadening behavior as a function of $\omega - \omega_0$. This assumption could not be tested rigorously, since no theoretical treatment of saturation broadening of the spread exists. However, in the present analysis we will utilize the Rabi frequency as evaluated in Ref. 11. The experimental interaction time, calculated for the most probable velocity of the longitudinal Maxwellian distribution, was long enough that the spread of the atomic beam was in the saturation region of the curves of Fig. 3. This was valid for most atoms in the velocity distribution, so that we assume that the spread of the atomic beam for any laser power density must be compared with the saturated, limiting value to which the curve in Fig. 3 tends as $t \rightarrow \infty$.

In Fig. 4 the experimental values of the spread of the atomic beam are reported together with the theoretical curve of OSGE obtained as discussed above, using the values of Ω reported in

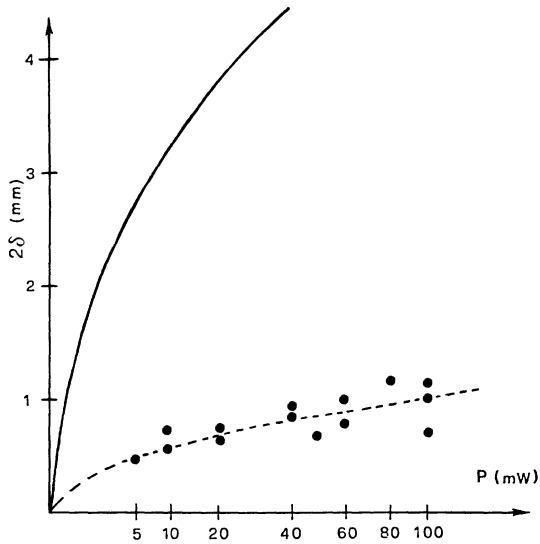


FIG. 4. Experimental data for the spread of the Na beam measured in Ref. 11; the dashed line passing through the experimental points has been reported in that reference. The continuous line is the theoretical curve of the OSGE. The scale on the abscissa axis is proportional to the square root of the applied laser power, i.e., the electric field amplitude.

Ref. 11. We see that the experimental values are less by a factor of ~ 4 than the theoretical ones, thus proving that the experiment cannot be interpreted as a pure OSGE.

On the other hand, in the experiment the coherence decay rate was smaller than the stimulated transition rates, which rules out the random walk model (see Appendix B) as a possible interpretation of the measured spread. Furthermore, the random walk model gives, as shown in Appendix B, a linear dependence of the spread on the electric field amplitude

$$\langle (b^2) \rangle^{1/2} \sim \mathcal{E}_0 \sqrt{\tau}, \quad (40)$$

which does not display the bend appearing in the experimental curve.

As we shall see in the next section, however, several additional effects, such as spontaneous emission processes or the Gaussian profile of the laser beam, combine to suppress the effective spread obtainable in actual experiments.

V. OTHER EFFECTS WHICH AFFECT THE SPREAD OF THE ATOMIC BEAM

We have also computed the quasiclassical OSGE with the inclusion of several other effects, namely: (i) spontaneous emission processes; (ii) a Gaussian profile of the laser beam; and (iii) misalignment of the atomic beam from the

normal incidence to the laser beam. These effects affect the spread of the atomic beam, and can reduce it by a factor of up to one order of magnitude.

A. Spontaneous emission processes

We show in Appendix A that spontaneous emission processes can be included in our model calculations. Their effect is to reduce the spread of the atomic beam, since they interrupt the coherence between translational and internal degrees of freedom, thus preventing the quanta of atomic momentum picked up from the field to add up coherently. We have numerically analyzed the simple case of the transit time comparable or shorter than the spontaneous lifetime $1/\gamma$, so that the stochastic function $\chi(t)$ can be replaced by its correlation function, as discussed in Appendix A. We report in Fig. 3, curves (c), (d), and (e), the spread obtained as a function of $\tau = \epsilon t$ for several values of $\gamma/4\epsilon$. The oscillations of the spread before reaching its saturated value are damped and, also, the final value is reduced considerably.

On Fig. 5 we report the saturated value of the spread as a function of the electric field amplitude for several values of $\gamma/4\epsilon$, for the typical conditions of the experiment on the Na beam of Ref. 11. The shape of the curves change when γ is increased until a situation is reached in which the spread becomes linear in the electric field amplitude [curve (d)] over the whole range of

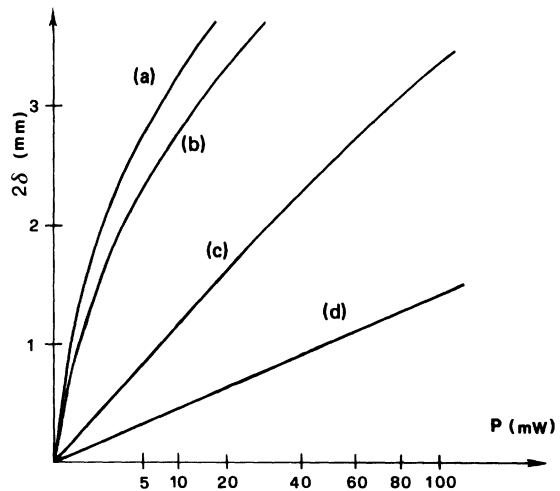


FIG. 5. Theoretical curves for the OSGE in the presence of a damping mechanism versus the laser power P in the typical conditions of the Na beam experiment. The curves (a), (b), (c), and (d) were obtained for $\gamma/4\epsilon = 0, 49, 200,$ and 500 , respectively. The scale on the abscissa axis is the same as in Fig. 4.

values of \mathcal{E}_0 reported. Thus, for large values of γ , we get the same linear dependence on \mathcal{E}_0 which we have obtained with the random walk model. However, even for those values of γ , if the electric field amplitude is increased (beyond the values reported in Fig. 5) the spread saturates again and approaches the value obtained in the absence of damping. Therefore, for large values of \mathcal{E}_0 all the curves in Fig. 5 would merge into the same curve.

B. Gaussian profile of the laser beam

Up to now, the electric field amplitude has been assumed constant in the interaction region, and zero elsewhere. However, under experimental conditions, the electric field amplitude varies smoothly across the laser beam, and an additional effect on deflection occurs. This effect can, in principle, either increase or decrease the spread of the atomic beam, depending on the experimental conditions. We have evaluated this additional effect just accounting for an electric field amplitude (or Rabi frequency Ω) which varies according to a Gaussian law across the beam, or, since the atoms traverse the light field with their longitudinal velocity which remains unaffected by the interaction with light, we have introduced a time-varying Rabi frequency Ω in Eqs. (33). The Gaussian beam waist and the peak amplitude of the field were chosen in such a way that the energy carried by both running waves was unchanged, and the time width of Ω was chosen to be equal to the interaction time of the square pulse shape used earlier. We have found that the spread of the atomic beam is significantly reduced when the square profile is replaced by a Gaussian shape. The reduction varies from 10% when $\Omega/\epsilon \sim 10^3$ to 40% when $\Omega/\epsilon \sim 2 \times 10^4$. These results have been obtained in the absence of relaxation. The saturated value of the spread vs the electric field amplitude maintains, after reduction, the same shape as in the case of square pulse profiles.

This behavior is interpreted observing that the much deflected particles have undergone a multiphoton process of very high order. The process depends on a very high power of the field distribution and hence the main contribution comes from the center of the laser Gaussian beam. For these particles the effective interaction time is greatly reduced and the spread of the atomic beam decreases.

C. Misalignment of the laser beam

If the angle between the longitudinal axis of the atomic beam and the direction of propagation of the laser beam is different from 90° by a small

amount, α say, then misalignment effects arise. Also this case can easily be treated in our model, since it is just necessary to integrate Eqs. (32) starting from an initial velocity different from zero and equal to the component of the undeflected atomic-beam velocity along the laser beam axis. We have evaluated this effect also with the inclusion of a damping rate γ in the same limits of validity discussed above in Sec. V A. The results are reported in Fig. 6. In the absence of relaxation ($\gamma = 0$) we have found that the atomic spread increases at small values of the misalignment angle α , because the initial atomic momentum in the x direction modifies the phase relation between the atomic wave function and the driving electric field. At large misalignment angles α , however, the spread is significantly reduced. Therefore, the maximum value of the spread is obtained for a value of α different from zero. When the relaxation mechanism is introduced, we see that it acts by reducing the spread for all values of α . Also, the enhancement of the spread at small values of α ($\neq 0$) tends to decrease, and eventually it disappears for increasing values of the damping constant γ .

VI. CONCLUSIONS AND DISCUSSION

We have shown that the quasiclassical limit of the OSGE contains its most important features and gives essentially the same results as the fully quantum-mechanical description. Those

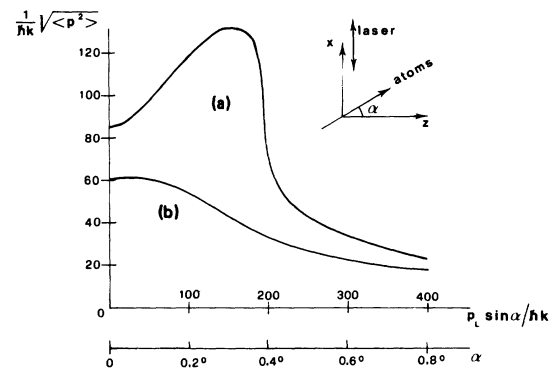


FIG. 6. Plot of the atomic momentum spread, in $\hbar k$ units and measured in the saturation regime, versus the misalignment parameter of the direction of the Na beam. In the lower abscissa axis the misalignment angle α is reported; in the upper abscissa axis the initial atomic momentum along the propagation direction of the laser beam is reported. Curve (a) is obtained in the absence of damping mechanism and curve (b) is obtained with $\gamma/4\epsilon = 98$. The Rabi flipping frequency is such that $\Omega/\epsilon = 4 \times 10^4$.

features which are lost in the passage to the quasiclassical limit are either not important or totally undetectable. Furthermore, the quasiclassical model can be worked out in a much simpler way than the quantum-mechanical model, and several additional effects which cannot be avoided under actual experimental conditions can be included in the model in a natural way.

Within our quasiclassical model we have also compared the behavior of the spread of the atomic momentum as a function of the electric field amplitude with the experimental data obtained recently by Arimondo *et al.*¹¹ for the spread of an atomic Na beam. We have found that the experimental results cannot be interpreted as a pure OSGE, since the observed spread is less by a factor of ~ 4 than the spread calculated with the quasiclassical model under the same conditions. On the other hand, the actual experimental conditions would force us to draw the same conclusion, since the complicating effects discussed in Sec. V could not be avoided and certainly had affected the observed spread. In particular, the interaction time of that experiment was long enough that phase-interrupting spontaneous emission processes were not negligible. Since the radiative damping occurs at a rate of $\gamma_u/4$, where γ_u^{-1} is the upper level radiation lifetime, an average number of 10 spontaneous emission processes occur during an interaction time. We have seen that these processes cause a net decrease of the spread, and this could bring the theoretical curve and the experimental results into better agreement. But this effect is by no means the only additional effect to the OSGE. Indeed, with a properly chosen value of γ , including other damping mechanisms, such as, for instance, laser fluctuation effects, an agreement with the experimental data could be obtained as an order-of-magnitude fit, but the theoretical curve would be a straight line [as a function of δ_0 ; see Fig. 5, curve (d), while the experimental points display a clear saturation behavior (see Fig. 4)]. Therefore, the other two effects mentioned in Sec. V must be affecting the observed spread. Unfortunately, the angle of misalignment of the geometrical configuration and the parameters of the Gaussian beam waist were not recorded with a sufficient degree of accuracy to justify a detailed fit to the experimentally observed spread.

ACKNOWLEDGMENTS

We wish to thank A. Bernhardt, R. J. Cook, and T. Oka for fruitful discussions and helpful suggestions. One of us (A.B.) is grateful to the Nordita Foundation for financial support.

APPENDIX A: INCLUSION OF SPONTANEOUS EMISSION PROCESSES IN THE QUASICLASSICAL MODEL OF OSGE

If we ignore the atomic motion and the interaction of translational degrees of freedom with the internal degrees of freedom, we can easily derive the rate of change of $\rho_{\alpha\alpha}$ and $\rho_{\beta\beta}$ caused by radiative damping of the upper level; we have

$$\dot{\rho}_{\alpha\alpha} = \frac{1}{2} + \frac{1}{2}(\rho_{ab} + \rho_{ba}), \quad (\text{A1})$$

$$\dot{\rho}_{\beta\beta} = \frac{1}{2} - \frac{1}{2}(\rho_{ab} + \rho_{ba}).$$

Denoting the rate of radiative damping of the upper level by γ , we therefore have

$$\dot{\rho}_{\alpha\alpha} = \frac{1}{2}(\dot{\rho}_{ab} + \dot{\rho}_{ba}) = -\frac{1}{4}\gamma(\rho_{ab} + \rho_{ba}), \quad (\text{A2})$$

$$\dot{\rho}_{\beta\beta} = -\frac{1}{2}(\dot{\rho}_{ab} + \dot{\rho}_{ba}) = +\frac{1}{4}\gamma(\rho_{ab} + \rho_{ba}),$$

or, in terms of $\rho_{\alpha\alpha}$ and $\rho_{\beta\beta}$

$$\dot{\rho}_{\alpha\alpha} = -\frac{1}{4}\gamma(\rho_{\alpha\alpha} - \rho_{\beta\beta}), \quad (\text{A3})$$

$$\dot{\rho}_{\beta\beta} = -\frac{1}{4}\gamma(\rho_{\beta\beta} - \rho_{\alpha\alpha}).$$

The inclusion of atomic recoil in the spontaneous emission process would modify Eqs. (A3).²³ However, we do not consider the change in the atomic momentum due to the spontaneous emission processes because we consider only the case where a few spontaneous processes occur, while the atoms undergo many induced ones. Furthermore, the momentum transferred to the atom in a spontaneous emission process has no privileged direction, so that its component along the x axis is negligible. Here the spontaneous emission processes are considered only in so far as they interrupt the phase of the coherent walkoff of the atom.

In the quasiclassical limit the momentum transferred in a spontaneous emission process is *a fortiori* negligible. Indeed, it is easy to see that when $\hbar k \rightarrow 0$, the damping is still described by the rhs of Eqs. (A3), with the density matrix elements evaluated at X, P .²³ The effect of spontaneous emission can therefore be described as a relaxation process in which α states turn into β states and β states into α states. Owing to this fact, each elementary spontaneous emission process inverts the sign of the force acting on the classical particle. If many elementary processes occur before the atom is appreciably displaced from its position $X(t)$, the force acting on it will average to zero; thus we recover the well-known result that the average force exerted by a classical standing-wave field tuned to resonance with the atomic transition is zero.²⁴

Fluctuations of the force around its average

value will cause the atoms to spread around the unperturbed trajectory $P = \text{const}$, in such a way as to leave unchanged the average transverse momentum. To describe this Brownian-type motion, we can write the stochastic equation of motion derived from (32):

$$m \frac{dX}{dt} = P, \quad (\text{A4})$$

$$\frac{dP}{dt} = \frac{\hbar k \Omega}{2} \chi(t) \sin kX,$$

where $\chi(t)$ is a stochastic function of t , which can assume only the values $+1$ and -1 . This function averages to zero

$$\langle \chi(t) \rangle = 0 \quad (\text{A5})$$

and is taken to have the correlation function

$$\langle \chi(t) \chi(t + \tau) \rangle = \exp(-\gamma \tau / 4). \quad (\text{A6})$$

This simple model is valid only if γ is smaller than the rate at which stimulated emission-absorption processes occur.

To obtain an estimate of the influence of the damping on the spread of atomic momentum in the case in which the laser beam is confined to a slab of finite thickness as discussed in Sec. II and the interaction time is comparable to or shorter than the spontaneous emission lifetime, we can replace the stochastic function $\chi(t)$ in (A4) with its correlation function (A6). The results of such a calculation are described in Sec. V A.

APPENDIX B: THE RANDOM WALK MODEL

We want to show here a method for evaluating the atomic momentum spread, under the assumption that the coherences of the internal states α, β and the translational ones have short lifetimes, compared with the average time interval between successive emission and absorption processes. In this case, the process is fully random—in contrast with the complete coherence of the process described in Sec. II—and we obtain a Markov random walk model. In this model it is not necessary that the photon momentum $\hbar k$ be small compared with the atomic momentum, as in the quasiclassical limit. It only requires a fast relaxation mechanism which destroys the coherences of the interaction process.

The random walk model can be evaluated as follows. Starting from $P = 0$ in the lower level, the atom acquires a momentum $P = \hbar k$ or $P = -\hbar k$ from the field, depending on which running wave has excited the atom to the upper level. Then a stimulated emission occurs, and the atom reaches

the momentum $P = 2\hbar k$ or $P = 0$ and $P = 0$ or $P = -2\hbar k$ depending on the momentum acquired in the absorption process. The atom is now again in the lower state, and the process goes on step by step (see Fig. 7).

The probability of reaching a certain momentum $n\hbar k$ after m steps, C_n^m , is proportional to the number of ways we can end up at this point, P_n^m . This probability distribution is easily seen to be given by the Pascal-Tartaglia triangle, i.e., $P_n^m = \binom{m}{|n|}$. The probabilities C_n^m , therefore, can be obtained from P_n^m after a proper normalization, and satisfies recurrence relations

$$C_n^{m+1} = \frac{1}{2}(C_{n+1}^m + C_{n-1}^m), \quad (\text{B1})$$

which is the mathematical formulation of the tree diagram of Fig. 7. Thus we have obtained the distribution of transverse momentum without the assumption that the photon momentum $\hbar k$ is small compared with P .

However, in the quasiclassical limit $\hbar k \rightarrow 0$, the relations (B1) assume a particularly appealing form. Writing (B1) using a second-order difference

$$C_n^{m+1} - C_n^m = \frac{1}{2}[(C_{n+1}^m - C_n^m) - (C_n^m - C_{n-1}^m)] \quad (\text{B2})$$

and taking the continuous limit, we find the diffusion equation

$$\frac{\partial C(m, n)}{\partial m} = \frac{1}{2} \frac{\partial^2 C(m, n)}{\partial n^2}, \quad (\text{B3})$$

where m now corresponds to the time t and n corresponds to the atomic momentum P . This shows the relationship with the Brownian motion. The diffusion equation (B3) can be solved easily, and gives for $C(m, n)$ a Gaussian distribution. Then the quasiclassical limit, in this case, is equivalent with the central limit theorem, according to which a binomial distribution tends towards a Gaussian distribution. The mean-

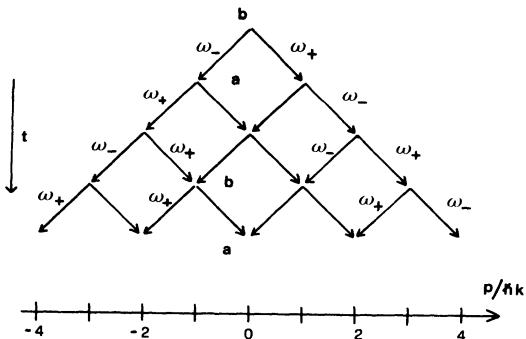


FIG. 7. Pascal-Tartaglia triangle representing schematically the time evolution of the atomic momentum in the random walk model.

square deviation of the Gaussian distribution is given by

$$\overline{n^2} = 2Dm = m. \quad (\text{B4})$$

Under the assumption specified above that the transition rate is taken to be proportional to E_0^2 and the interaction time is denoted by τ , (B4)

implies

$$\langle P^2 \rangle = CE_0^2 \tau, \quad (\text{B5})$$

where C is a constant. The present diffusion approximation is equivalent with a simplified version of the Fokker-Planck approach of the last reference in Ref. 16.

¹A. Ashkin, Phys. Rev. Lett. 24, 156 (1970); 25, 1321 (1970); A. F. Bernhardt, D. E. Duevre, J. R. Simpson, and L. L. Wood, Appl. Phys. Lett. 25, 617 (1974); A. F. Bernhardt, Appl. Phys. 34, 19 (1976); G. A. De-lone, V. A. Grinchuk, A. P. Kazantsev, and G. J. Sur-dutovich, Opt. Commun. 25, 399 (1978).

²T. W. Hänsch and A. L. Schalow, Opt. Commun. 13, 68 (1975); V. S. Letokhov, V. G. Minogin, and B. D. Pavlik, *ibid.* 19, 72 (1976); V. S. Letokhov, V. G. Minogin, and B. D. Pavlik, Zh. Eksp. Teor. Fiz. 72, 1328 (1977) [Sov. Phys.—JETP 45, 698 (1977)].

³M. Bloom, E. Enga, and H. Lew, Can. J. Phys. 45, 1481 (1967).

⁴R. M. Hill and T. F. Gallagher, Phys. Rev. A 12, 451 (1975).

⁵J. E. Bjorkholm, R. R. Freeman, A. Ashkin, and D. B. Pearson, Phys. Rev. Lett. 41, 1361 (1978); *Proceedings of the Fourth International Conference on Laser Spectroscopy, Rottach-Egern, 1979*, edited by H. Walther and K. W. Rothe (Springer, Berlin, 1979).

⁶A. C. Tam and W. Happer, Phys. Rev. Lett. 38, 278 (1977); *Proceedings of the Third International Conference on Laser Spectroscopy, Jackson Lake Lodge, 1977*, edited by J. L. Hall and J. L. Carlsten (Springer, Berlin, 1978).

⁷O. R. Frisch, Z. Phys. 86, 42 (1933).

⁸R. Schreder, H. Walther, and L. Woste, Opt. Commun. 5, 337 (1972); J. L. Picque and J. L. Vialle, *ibid.* 5, 402 (1972); J. E. Bjorkholm, A. Ashkin, and D. B. Pearson, Appl. Phys. Lett. 27, 534 (1975); N. D. Blaskar, B. Jadaszliwer, and B. Bederson, Phys. Rev. Lett. 38, 14 (1977); see also A. F. Bernhardt *et al.*, Ref. 1.

⁹D. J. Wineland, R. E. Drullinger, and F. L. Walls, Phys. Rev. Lett. 40, 1639 (1978); W. Neuhauser, M. Hostenstatt, P. E. Toschek, and H. G. Dehmelt, *ibid.* 41, 233 (1978); *Proceedings of the Fourth International Conference on Laser Spectroscopy Rottach-Egern, 1979*, edited by H. Walther and K. W. Rothe (Springer, Berlin, 1979), p. 73; R. E. Drullinger

and D. J. Wineland, *ibid.*, p. 66.

¹⁰For a recent review on the Kapitza-Dirac effect and experiment, see Y. W. Chan and W. L. Tsui, Phys. Rev. A 20, 294 (1979).

¹¹E. Arimondo, H. Lew, and T. Oka, Phys. Rev. Lett. 43, 753 (1979); *Proceedings of the Fourth International Conference on Laser Spectroscopy, Rottach-Egern, 1979*, edited by H. Walther and R. W. Rothe (Springer, Berlin, 1979), p. 56.

¹²V. S. Letokhov and B. D. Pavlik, Appl. Phys. 9, 229 (1976); V. S. Letokhov and V. Minogin, Phys. Lett. A 61, 370 (1977); Zh. Eksp. Teor. Fiz. 74, 1318 (1978) [Sov. Phys.—JETP 47, 690 (1978)]; Appl. Phys. 17, 99 (1978); J. Opt. Soc. Am. 69, 413 (1979); see also Ref. 2.

¹³For a review see A. P. Kazantsev, Usp. Fiz. Nauk. 124, 113 (1978) [Sov. Phys. Usp. 21, 58 (1978)].

¹⁴J. L. Picque, Phys. Rev. A 19, 1622 (1979).

¹⁵R. J. Cook and A. F. Bernhardt, Phys. Rev. A 18, 2533 (1978).

¹⁶S. Stenholm, Appl. Phys. 15, 287 (1978); Phys. Rep. C43, 151 (1978); S. Stenholm, V. G. Minogin, and V. S. Letokhov, Opt. Commun. 25, 107 (1978); S. Stenholm and J. Javanainen, Appl. Phys. 16, 159 (1979).

¹⁷R. J. Cook, Phys. Rev. Lett. 41, 1788 (1978); Phys. Rev. A 20, 224 (1979); 21, 268 (1980); Phys. Rev. Lett. 44, 976 (1980).

¹⁸R. J. Cook, Phys. Rev. A 22, 1078 (1980).

¹⁹J. P. Gordon and A. Ashkin, Phys. Rev. A 21, 1606 (1980).

²⁰P. Knight, Nature 278, 14 (1979); see also Refs. 3, 4, and the first paper by Cook in Ref. 17.

²¹A. Bambini and S. Stenholm, Opt. Commun. 25, 244 (1978); 30, 391 (1979); A. Bambini, A. Renieri, and S. Stenholm, Phys. Rev. A 19, 2013 (1979).

²²A derivation of Eqs. (16) is given in Ref. 15.

²³See the first reference in 16 for a detailed treatment.

²⁴See, for instance, the second paper by Cook in Ref. 17.